ISSN: 2472-3703 DOI: 10.6911/WSRJ.202304_9(4).0031

Migration Characteristics of Leaching Solution in Uranium Formation with CO_2+O_2 In-situ Leaching: A Case from Coal-Uranium Co-mining Ore in Ordos Basin, China

Xin Yang[1, 2, a]

[1]State Key Laboratory of Mining Response and Disaster Prevention and Control in Deep Coal Mines, Anhui University of Science & Technology, Huainan 232001, China

[2]School of mining, Anhui University of Science & Technology, Huainan 232001, China

[a]2673733989@qq.com

Abstract

The co-mining of coal and uranium resources is directly related to the environment. The vertical migration of uranium leaching solution in underground leaching threatens the safety of coal mining, and the mining changes the efficiency of uranium leaching. Based on a coal-uranium co-occurrence deposit in the Ordos Basin, a 3D numerical model of CO2+O2 in-situ leaching of uranium under different coal-uranium mining sequences was constructed using the mineralized analysis software TOUGHREACT. The transport and diffusion of the leaching solution, the chemical reaction between the leaching solution and reservoir minerals, and the leaching efficiency of uranium ore were simulated at different leaching times. The results show that the mining time of uranium coal affects the spatial distribution of uranium-containing leaching solution. In the fifth year of simulation, the migration range of the leaching solution in the preferential coal mining model reached the level of the 20th year in the preferential uranium mining model. In the 20th year of simulation, the leaching solution diffused to the horizontal boundary of the preferential coal mining model and migrated to 17 m above the coal seam in the vertical direction. The maximum migration depth of the preferential coal mining model is increased by 33 m, forming a "tripod" migration field. The uranium recovery rates of the two models show the same trend with time. The uranium content in 0-8 years leaching solution is the highest, and the uranium content in 8-20 years decreases to the lowest level. This study can provide technical support for multi-resource safe and coordinated mining as well as forecast coal mining safety threats in advance.

Keywords

Coal-uranium; In-leaching; TOUGHREACT; Migration; Mineral reaction.

1. INTRODUCTION

Over the years, many sizeable sandstone-type uranium deposits have been discovered near the coal mines in the Erdos area, Inner Mongolia, China, which have been transformed from single-resource mining to multi-resource coordinated development [1-4]. Based on the analysis of the essential characteristics of coal and uranium co-associated mining areas and the mining experience of this type of deposit, it is considered that the mining sequence of coal before uranium will form a water-conducting fissure above the coal seam and increase the diffusion range of uran-containing leaching solution in the vertical direction. The mining mode of uranium before coal will also form an uran-containing leaching solution and directly affect

ISSN: 2472-3703 DOI: 10.6911/WSRJ.202304_9(4).0031

whether the coal mine can continue to be mined [5-9]. Some scholars have begun to pay attention to the problem of the mutual response of coal and uranium resource mining.

The transport of groundwater pollutants in the process of uranium leaching is correlated with the geology and fluid flow, Martin et al. [10] established one, two, and three general surface uranium transport models in PHREEQC using the generalized composite surface complex model (GC SCM) and predicted the transport characteristics of uranium in sediments composed of uniform minerals. Nguyen et al. [11] mapped the concentration distribution of all substances related to the reaction mechanism, and the effects of the quality of the leaching solution, initial conditions, and migration conditions on the leaching products were investigated. Fu et al. [12] studied the U adsorption and transport behavior of typical red soil in southern China through batch adsorption and column experiments, considering the initial PH and carbonate concentration of electrolyte solution with high sulfate background. Windt et al. [13] used the reaction transport model to simulate the oxidative dissolution of uranium dioxide (UO_2) and the subsequent migration of uranium in the underground environment and underground waste disposal. Yabusaki et al. [14] analyzed data from a 2002 field experiment using a multi-component reactive transport model to identify the main transport and biological processes controlling uranium migration during biostimulation and to determine field-scale parameters for these simulated processes. Zhang et al. [15] studied the reaction transport model of uranium (VI) contaminated sediment column with alkali added to circulating influent water and found that with the increase of PH value, the adsorption of U(VI) by slowly precipitated Al can be effectively isolated. Phillippi et al. [16] combined strongly interacting solutes [U(VI) and carbonate] and adsorbents [Fe(III) oxygen hydroxides] with single-component solutes or adsorbents adsorption isotherms independent of the solid/liquid ratio. They found that this would lead to multi-component systems where the adsorption isotherms became dependent on the solid/liquid ratio. Curtis et al. [17] used the surface complexation model (SCM) to simulate the reaction transport process of U(VI) in shallow alluvial aquifers, described the adsorption process of U(VI), and found that the reaction transport simulation results were consistent with the observed U(VI) and alkalinity. Most of these studies only consider fluid migration in the horizontal direction of the formation but lack research on the migration and diffusion law perpendicular to the formation direction.

The coal mining beneath the aquifers concerns mining safety and environmental protection, Lu et al. [18] proposed a coupling simulation method of damage and flow based on micromechanics, which simulated the gradual development of fractures in floor rock strata and the associated water flow during the mining process of confined aquifers. Meng et al. [19] combined the characteristics of geological heterogeneity, working face displacement, and underground borehole extraction principle into the covert borehole drainage optimization model. They proposed a new mathematical model including these three characteristics. Karaman et al. [20] developed a method based on one-dimensional seepage equations. They used type curves to estimate aquifer hydraulic diffusivity values from individual well water level measurements over time, predicting mine-induced water level decline. Zhang et al. [21] monitored overburden failure, loose aquifer water level, surface cracks, and land subsiding in a series of boreholes. They found that water conservation mining technology can be successfully applied if a few mining parameters, such as mining height or feed rate, are modified under certain conditions. Zhang et al. [22] observed the change in aquifer groundwater level when the longwall working face crossed the belt. Zhai et al. [23] took time-varying Bingham slurry as the research object, studied the slurry diffusion mechanism in the horizontal fracture of the fractured aquifer, and established a one-dimensional theoretical model of see-through grouting considering the spatiotemporal variation of slurry viscosity at a constant grouting rate. Fan et al. [24] found that the underground aquifer or surface water can be protected by controlling the movement of key rock layers, ensuring the appropriate interlayer thickness, and protecting the

ISSN: 2472-3703 DOI: 10.6911/WSRJ.202304_9(4).0031

natural water barrier. Zhang et al. [25] studied the seepage characteristics and mechanism of fault water inrush above confined aquifer in coal mining and designed a simulation model of fault water inrush. In terms of the research on the coordinated mining of coal and uranium. Cui et al. [26] selected the permeability evolution of the rock around the coal seam as the key parameter indicating the safe separation and simultaneous mining of the two deposits, proposed a new strain-related permeability model covering the whole deformation range of rocks, and studied the feasibility of the combined mining of coal seam and uranium deposit. Some scholars used FLAC3D-CFD(fluent) simulation software to visually analyze the mining response law under the stress-fracture-seepage field coupling using the non-Darcy model and analyzed the dynamic characteristics under the condition of multi-field coupling. Using the fast Lagrange analysis method of continuous computational fluid dynamics, The evolution law and morphological characteristics of multi-field coupling of mining are studied under two scenarios of simultaneous coal and uranium mining and asynchronous mining [27, 28]. Physical experiments on transparent soil were also carried out to characterize liquid and solid migration characteristics in resource co-occurring ore areas [29]. However, mining uran-coal resources involve complex physical and chemical changes, among which the diffusion and transport law of leaching solution under the coupling condition of seepage and chemical fields is rarely studied.

In this study, the CO_2+O_2 neutral leaching uranium was performed, as an example, in a coal-uranium resource co-occurrence mining area in the Ordos Basin, China. Based on the simulation software TOUGHREACT, considering the complete coupling process of the see-chemical field, a three-dimensional numerical model of the reaction transport of CO_2+O_2 in in-situ leaching of uranium is established. The dynamic leaching process simulation of uranium ore under different mining time sequences is carried out. The migration characteristics of the leaching solution in the vertical formation direction of different mining sequence models are intensely analyzed. The law of chemical dissolution precipitation of reservoir minerals and the leaching efficiency of uranium ore in different models were found. It provides reference and technical support to ensure multiple resources' safe and coordinated exploitation.

2. GEOLOGICAL CONDITION

2.1. Geological characteristics

The middle and Cenozoic Triassic (T), Jurassic (J), Lower Cretaceous (K1), Neoproterozoic Pliocene (N2), and Quaternary (Q) cover the northern, eastern part of Ordos Basin. The Triassic, Jurassic, and Cretaceous are the basin's central bodies of sedimentary cover. The Middle Jurassic Zhiluo Formation is the primary uranium ore-forming layer in the region, and the Middle Jurassic Yan'an Formation is the active exploration layer for uranium ore search (Fig. 1). According to the changes in geologic climate and lithological development characteristics during the deposition period of the Zhiluo Formation, it is divided into an upper section (J2z2) and a lower section (J2z1). It can further divide the lower area into an upper sub-section (J2z1-2) and a lower sub-section (J2z1-1). The lower sub-section of the lower section of the Straight Law Group (J2z1-1): The lower sub-section of the lower section of the Straight Law Group is a braided river depositional system in the early stage of deposition under a humid climate, with a gravelly braided river depositional system at the bottom and a sandy braided river depositional system in the upper transition, which is characterized by sand bodies appearing primarily in the position of deep-cut valleys and having the depositional characteristics of filling in and filling out. The upper sub-section of the lower section of the Zhengluo Group (J2z1-2): The upper sub-section of the lower section of the Zhengluo Group is a set of the quicksilver-quicksilver deltaic sedimentary system under the humid climate. The sand body in the upper

ISSN: 2472-3703 DOI: 10.6911/WSRJ.202304_9(4).0031

sub-section is striped, with significant phase change and limited distribution, featuring a more developed floodplain and prominent "binary structure."

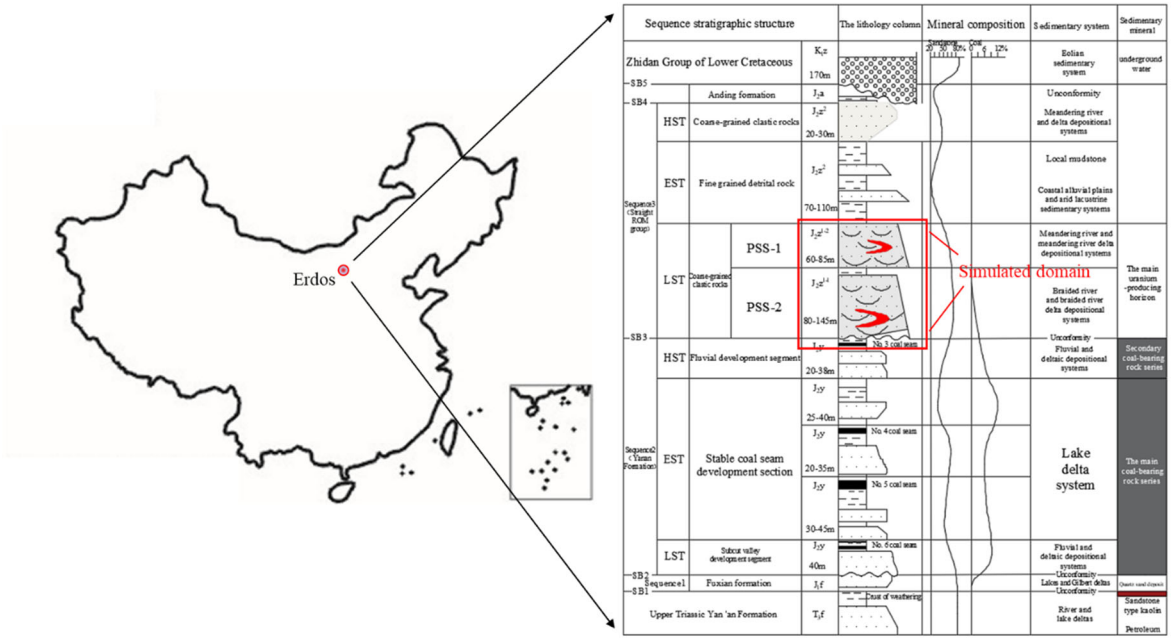

Figure 1. Stratigraphic bar chart of a coal-uranium deposit in Ordos area

2.2. Hydrogeological characteristics

Middle Jurassic Zhiluo Formation (J2z) pressurized water aquifer: The uranium ore-bearing aquifer of this study. This water-bearing rock group is subducted under the Lower Cretaceous water-bearing rock group, with stable distribution and a relatively simple hydrogeological structure. The groundwater type is interstratified pressurized water. The lithology is mainly composed of green and gray medium sandstone, medium and coarse sandstone, and coarse sandstone in the river phase, with thin mudstone and siltstone, good water-richness, and permeability. The water table depth is 109.45~153.41m, and the head of water under pressure is 169.55~252.46m. The water table elevation and head of water under pressure of the mineral-bearing aquifer have the characteristics of gradually increasing from north to south.

3. CHEMICAL REACTION MODEL

3.1. Multifield reaction equation

CO_2+O_2 in situ leaching of uranium means that under the natural burial condition of uranium deposit, the leaching solution (H_2O+CO_2+O_2) prepared in a particular proportion is injected into the target reservoir through the injection hole. CO_2 is the primary reaction solvent in the leaching process, and O_2 is the oxidant to oxidize n-tetravalent uranium into n-hexavalent uranium in the ore layer. Then it reacts with HCO_3^- to form uranyl carbonate ion, which stably exists in the solution. In the process of in-situ leaching, there will be complex interactions between the leaching solution and orebody, including oxidation-reduction, dissolution-precipitation, complexity-dissociation, and other water-rock interactions between the leaching solution and uranium ore and surrounding rock. The main chemical reactions involved are shown in Table 1 [30, 31]. The hydrolysis and carbonate complexation reactions associated with uranyl ions and their equilibrium constants used in the numerical calculations of TOUGHREACT are summarized in the table, and the relevant responses are derived from the llnl.dat database and the ThermoChimie thermodynamic database.

ISSN: 2472-3703 DOI: 10.6911/WSRJ.202304_9(4).0031

Table 1. Main chemical reactions and thermodynamic data of uranium leaching process

Serial number	Chemical equation	Reaction equilibrium constant/LogK(25℃)
1	$CO_2 + H_2O=2H^+ + CO_3^{2-}$	-16.680
2	$H^+ + CO_3^{2-} = HCO_3^-$	10.330
3	$UO_2+4H^+=U^{+4}+2H_2O$	-4.850
4	$U^{4+}+0.5O_2+2H_2O=UO_2^{2+}+2H^+$	33.955
5	$UO_2^{2+}+2CO_3^{2-}=UO_2(CO_3)^{2-}$	16.610
6	$UO_2^{2+}+3CO_2^{2-}=UO_2(CO_3)^{-4}$	21.840
7	$UO_2+0.5O_2+2HCO_3^-=UO_2(CO_2)_2^{2-}+H_2O$	25.055
8	$UO_2+0.5O_2+3HCO_3^-=UO_2(CO_3)_3^{4-}+H_2O^+H^+$	19.955
9	$2UO_2^{2+}+2H_2O=(UO_2)_2(OH)_2^{2+}+2H^+$	-5.62
10	$3UO_2^{2+}+4H_2O=(UO_2)_3(OH)_4^{2+}+4H^+$	-11.90
11	$2UO_2^{2+}+CO_3^{2-}+3H_2O=(UO_2)_2CO_3(OH)_3^-+3H^+$	-0.86
12	$3UO_2^{2+}+CO_3^{2-}+3H_2O=(UO_2)_2CO_3(OH)_3^++3H^+$	0.66

3.2. Governing equation

In this study, the ECO2N module in TOUGHREACT was used for simulation, the integrated finite difference method (IFDM) was used to discolor the space, and the sequential iteration method was used to solve the equations of multiphase seepage flow, solute transport, and chemical reaction. Multiphase fluid and heat flow met the fundamental conservation of mass and energy, and the governing equations were expressed as follows [32, 33]:

$$\frac{\mathrm{d}}{\mathrm{d}t}\int M^{\kappa}\mathrm{d}V_n = \int \mathrm{F}^{\kappa}\cdot \mathrm{n}\mathrm{d}I_n + \int q^{\kappa}\mathrm{d}V_n \tag{1}$$

Where: V_π is any integrator region, Γ_n is the surface of the integral region, M is the mass or energy per unit volume (κ=1,... , NK represents different components, such as water, air, solute, etc., κ=NK+1 represents energy), F is the pair flow of mass and heat, q represents the source and sink term, and n is the rate vector of the surface of the integrated region.The seepage velocity is calculated by Darcy's law, as [34, 35]:

$$v_\beta = -k\frac{k_{r\beta}}{\mu_\beta}\left(\nabla P_\beta - \rho_\beta g\right) \tag{2}$$

Where: v_β is Darcy flow velocity (m/s), K is intrinsic permeability (m^2), $k_{r\beta}$ is relative permeability, μ_β is dynamic viscosity (m^2/s), P_β is fluid pressure (Pa), G is gravitational acceleration (m/s^2).

The governing equation for multi-component solute transport is [36, 37]:

$$\frac{\partial M_i}{\partial t} = -\nabla F_i + q_i (i = 1,2,3,\dots N) \tag{3}$$

$$M_i = \emptyset S C_i \tag{4}$$

$$F_i = uC_i - (\tau\varphi SD)\nabla C_i \tag{5}$$

ISSN: 2472-3703 DOI: 10.6911/WSRJ.202304_9(4).0031

Where: ϕ is porosity, S is liquid phase saturation, C_i is concentration of the i species component in liquid phase (mol/L), τ is curvature coefficient of aqueous medium, D is diffusion coefficient (m^2/d), q_i the source and sink term of the i species component, including water chemical reaction term.

4. ESTABLISHMENT OF NUMERICAL MODEL

4.1. Model overview

This simulation area mainly focuses on the dynamic leaching process of eight in-situ leaching units in the mining area. Considering the operation speed and calculation amount of numerical simulation, only the main uranium seam PSS-1 and No.3 coal seam are se lected as the reference area of the numerical model. During the simulation, the complex process of fluid flow-chemical reaction coupling in different mining sequences of coal and uranium resources was identified and then extended to the whole mining area. The size of the numerical model was selected as 300m×180m×150m, the calculation unit was divided according to the form of an irregular polyhedron, and the grid encryption was carried out around the pumping hole and injection hole. Among them, the geometric model of the whole mining area is shown in Fig. 2, and the naming and distribution of the blooming pattern are shown in Fig. 3. There are 23 ground immersion drilling holes, including 15 injection Wells and eight pumping Wells, forming a "five-point type" ground immersion unit with four injections and one pumping.

Two geometric numerical models are designed in this simulation to optimize the coordinated mining process in the coal-uranium overlapping area. One of them is the mining mode of uranium first and coal second, which is mainly set up with a uranium ore layer (30m), sandstone aquifer (90m), and coal and mudstone formations (30m). The scheme is mainly designed to carry out in-situ leaching mining of uranium ore when the coal seam below is not excavated. The migration law of uranium leaching solution in the aquifer and the physicochemical changes of CO_2 injection and formation minerals were simulated during the in-situ leaching process. The other scheme is the mining mode of coal before uranium, which is mainly set up with a uranium ore layer (30m), sandstone aquifer 1 (30m), sandstone aquifer 2 (30m), sandstone aquifer 3 (30m), coal and mudstone caveated bed (30m). The scheme is mainly designed to carry out coal seam excavation before uranium ore leaching mining. At the end of coal seam mining, "three zones" (caving zone, fracture zone, and bending subsiding area) are formed. At this time, the porosity and permeability of the surrounding rock under the uranium ore layer change with the generation of fractures, which simulates the migration law of uran-containing leaching solution in the vertical direction of the formation its influence on the continued development of the coal mine area.

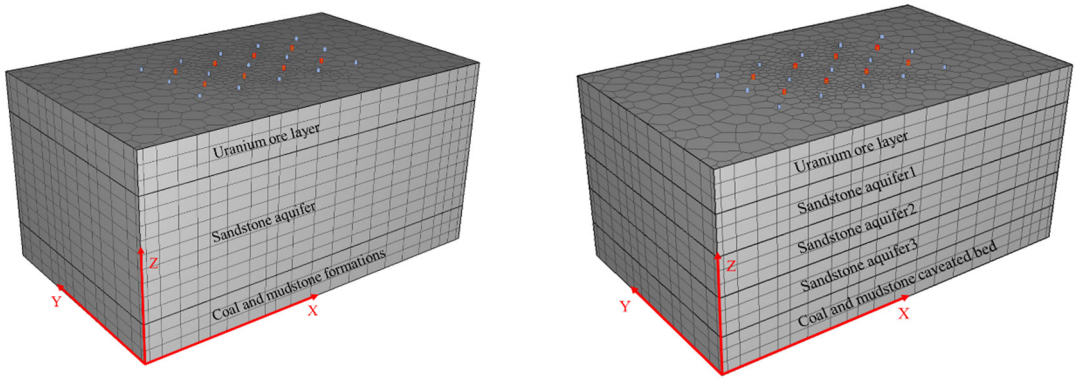

(a)Preferential uranium mining model (b)Preferential coal mining model

Figure 2. Three dimensional geological model of different mining sequences

ISSN: 2472-3703 DOI: 10.6911/WSRJ.202304_9(4).0031

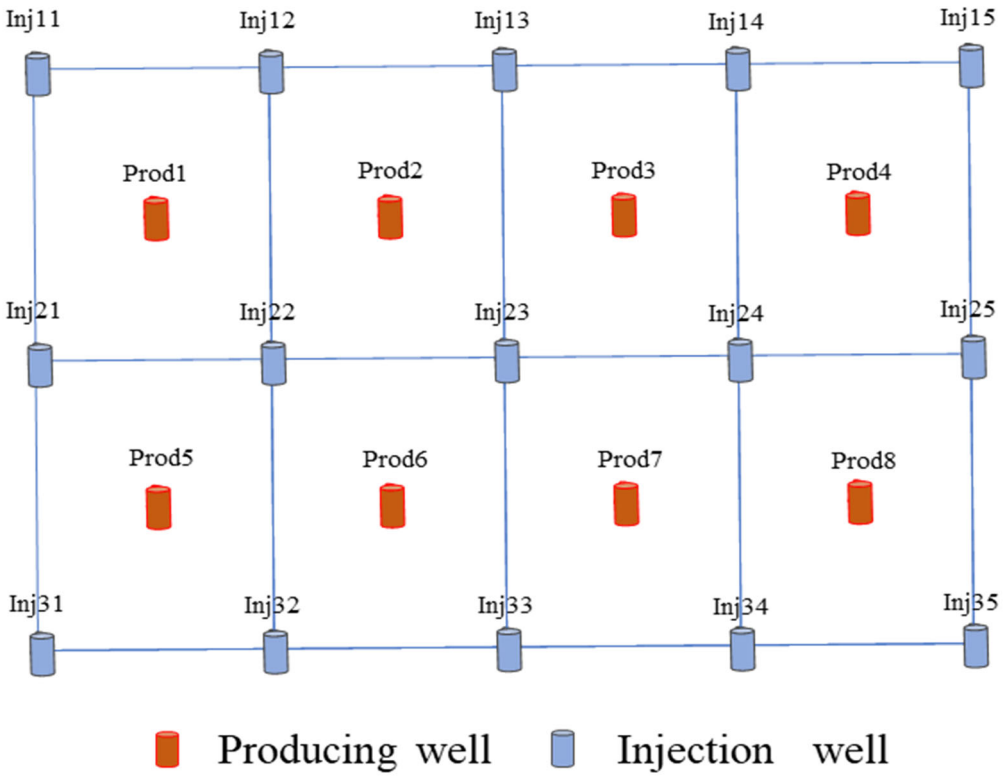

Figure 3. Five-point ground immersion unit

The pumping and injection wells are all arranged in the uranium ore layer, in which the flow rate of the pumping well is set to 1.8kg/s, and the flow rate of the injection well is set to 0.8kg/s. The ratio of CO_2 to H_2O in the leaching solution is 7:1. Due to the software's limitation, groundwater's dissolved oxygen content is set to 800mg/L in advance to replace the O_2 injection. The two models' upper and lower boundaries and the left and proper boundaries are set as no-flow boundaries. The hydrodynamic parameters used in the models are shown in Table 2 and 3, respectively. Due to the lack of empirical formulas for the height of "three zones," the porosity permeability of the preferential coal mining model is challenging to be accurately defined, so empirical values are taken according to the studies of relevant researchers [38-41]:

Table 2. Hydrodynamic parameters of uranium before coal model [38-41]

Hydrodynamicparameter	Uranium ore layer	Sandstone aquifer	Coal and mudstone formations
Porosity	0.25	0.25	0.025
Rock grain density(kg/m^3)	2500	2400	2100
XY direction permeability(m^2)	1×10^{-13}	1×10^{-13}	1×10^{-15}
Z direction permeability(m^2)	5×10^{-14}	5×10^{-14}	5×10^{-16}
Temperature(°C)	25	25	25
Pore Compressibility(Pa^{-1})	4.5×10^{-10}	4.5×10^{-10}	4.5×10^{-10}
Diffusion coefficient(m^2·s^{-1})	1.0×10^{-9}	1.0×10^{-9}	1.0×10^{-9}

ISSN: 2472-3703 DOI: 10.6911/WSRJ.202304_9(4).0031

Table 3. Hydrodynamic parameters of coal before uranium model [38-41]

Hydrodynamicparameter	Uranium ore layer	Sandstone aquifer1	Sandstone aquifer2	Sandstone aquifer3	Coal and mudstone caveated bed
Porosity	0.25	0.3	0.35	0.4	0.5
Rock grain density(kg/m^3)	2500	2400	2400	2400	2100
XY direction permeability(m^2)	1×10^{-13}	1.0×10^{-12}	1.0×10^{-11}	1×10^{-10}	1×10^{-10}
Z direction permeability(m^2)	5×10^{-14}	5×10^{-13}	5×10^{-12}	5×10^{-11}	5×10^{-11}
Temperature(°C)	25	25	25	25	25
Pore Compressibility(Pa^{-1})	4.5×10^{-10}	4.5×10^{-10}	4.5×10^{-10}	4.5×10^{-10}	4.5×10^{-10}
Diffusion coefficient(m^2·s^{-1})	1.0×10^{-9}	1.0×10^{-9}	1.0×10^{-9}	1.0×10^{-9}	1.0×10^{-9}

4.2. Mineral composition

The results of scanning electron microscope and X-ray diffraction experiments on the core samples of the borehole show that the uranium minerals are mainly pitchblende. The main minerals in the rock samples were quartz (39.22%), albite (2.17%), K-feldspar (4.57%), and calcite (0.48%), followed by clay minerals (53.56%). Clay minerals mainly include kaolinite, illite, and plagiochlorite, of which plagiochlorite (32.35%) is the most developed, followed by kaolinite (16.97%) and illite (4.24%). Uranium-bearing minerals are mainly adsorbed in the gap of quartz particles or on the surface of clay minerals. Mineral parameters in the reaction transport model are defined in Table 4.

Table 4. Mineral parameters in the reaction transport model

Mineral name	Chemical formula	Volume fraction(%)	Reaction specific surface area(cm^2/g)
Quartz	SiO_2	39.22	9.8
Clinochlore	$(Mg,Fe)_{4.75}Al_{1.25}(Al_{1.25}Si_{2.75}O_{10})(OH)_8$	32.55	9.8
Kaolinite	$Al_2Si_2O_5(OH)_4$	16.97	151.63
K-feldspar	$KAl_3O_6Si_3O_8$	4.57	9.8
Illite	$K_{0.65}\{Al_2[Al_{0.65}Si_{3.35}O_{10}](OH)_2\}$	4.24	151.63
Albite	$NaAl_3Si_3O_8$	2.17	9.8
Calcite	$CaCO_3$	0.48	53.96
Pitchblende	UO_2	0.05	1100

4.3. Chemical composition of groundwater

Through the detection of the total ion component content of aquifer water samples in the mining area, the primary ion components of aquifer and leaching solution were selected as the customized variables of the reactive solute transport model, including H_2O, H^+, Ca^{2+}, Mg^{2+}, Na^+, K^+, Fe^{2+}, HCO_3^-, SO_4^{2-}, AlO_2^-, Cl^-, $SiO_2(aq)$, $O_2(aq)$, where the associated aqueous complex and the equilibrium constant are defined in the thermodynamic database. The customized chemical component information is shown in Table 5.

5. RESULTS AND ANALYSIS

5.1. CO_2 transport

As the primary reaction solvent in the in-situ leaching process, CO_2 is one of the main factors affecting the leaching efficiency of uranium ore. After the injection of CO_2 aqueous solution into the formation, due to the dual influence of formation pressure and formation temperature, CO_2

ISSN: 2472-3703 DOI: 10.6911/WSRJ.202304_9(4).0031

can easily reach the supercritical state. Therefore, different forms of CO_2 are analyzed in the simulation results.

Table 5. Initial concentration of aquifer chemical components

Chemical constituents	Concentration(mol/kg)	Chemical constituents	Concentration(mol/kg)
H_2O	1.0000	HCO_3^-	0.1841×10^{-2}
H^+	0.8480×10^{-7}	SO_4^{2-}	0.1443×10^{-15}
Ca^{2+}	0.4479×10^{-2}	AlO_2^-	0.1078×10^{-7}
Mg^{2+}	0.2348×10^{-4}	Cl^-	0.9109
Na^+	0.9006	$SiO_2(aq)$	0.9203×10^{-3}
K^+	0.5805×10^{-2}	$O_2(aq)$	0.0250
Fe^{2+}	0.2615×10^{-6}		

5.1.1 Liquid CO_2 transport

In the first year of simulation, the diffusion range of liquid CO_2 in the two models was almost the same. The deepest diffusion reached about 20m below the uranium layer (Fig. 4, Fig. 5). Since the eight pumping Wells are mainly distributed in the simulation area, the pumping Wells will also extract part of CO_2 when the injection Wells inject the CO_2 containing leaching solution. It can be seen that the regions with large liquid CO_2 mass fraction in the

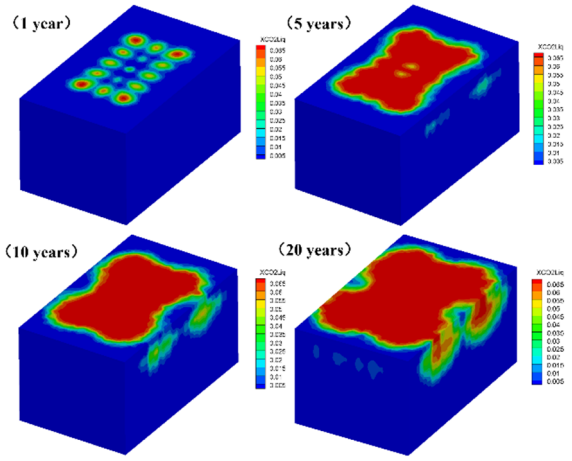

(a)Preferential uranium mining model

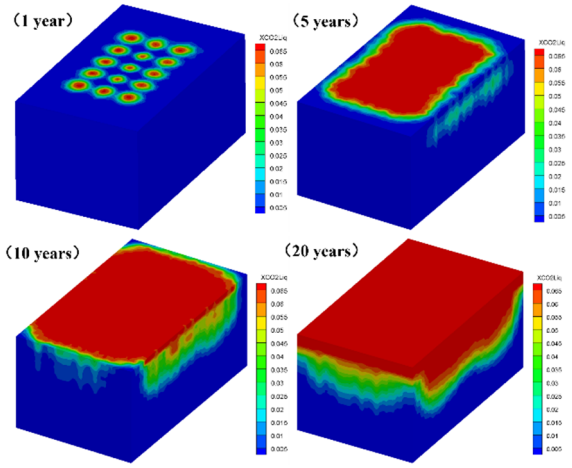

(b)Preferential coal mining model

Figure 4. Mass fraction of liquid CO_2 in water in different models

ISSN: 2472-3703 DOI: 10.6911/WSRJ.202304_9(4).0031

aquifer are concentrated in the periphery of the excellent network, and the diffusion speed and diffusion range of liquid CO_2 in the middle region are smaller than those in the periphery region (Fig. 5). In the preferential uranium mining model, the diffusion range of liquid CO_2 does not change significantly from the 5th year to the 10th year. Still, it reaches the maximum diffusion range in the 20th year. The horizontal diffusion range is close to the model boundary. The maximum vertical migration depth reaches 45m below the uranium seam, which is still 45m away from the coal seam below. In the preferential coal mining model, the diffusion range of liquid CO_2 reached the maximum diffusion range in the preferential uranium mining model in the fifth year. By the 20th year of simulation, liquid CO_2 has spread to cover the entire

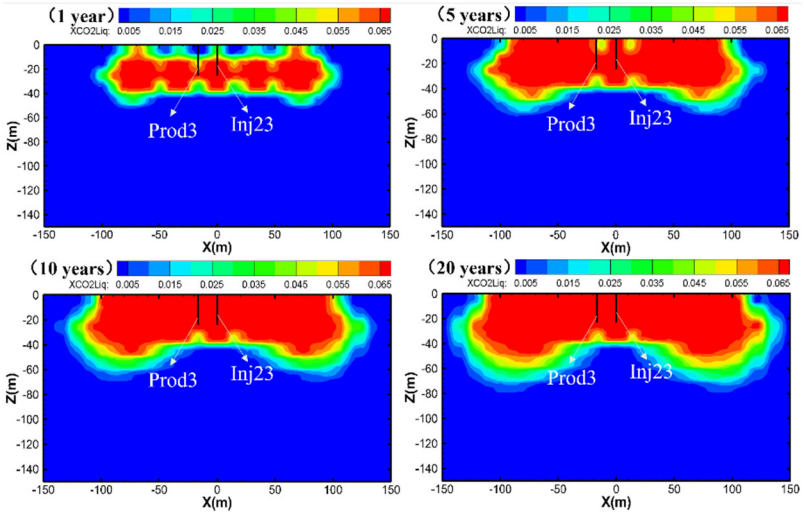

(a)Preferential uranium mining model

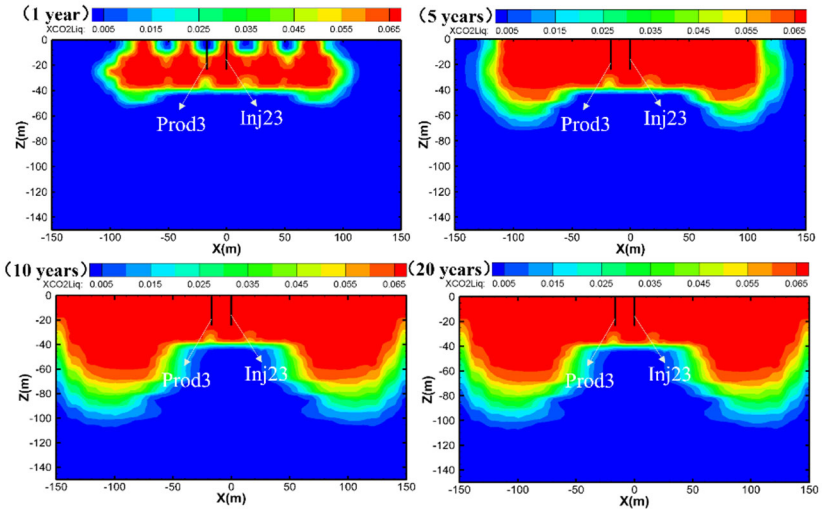

(b)Preferential coal mining model

Figure 5. Mass fraction of liquid CO_2 in water Y=90m profile in different models

uranium ore layer, and the maximum vertical migration depth has reached 75m below the uranium ore layer, which is only 15m from the coal seam below. Compared with the preferential uranium mining model, the maximum vertical migration depth is increased by 30m. By comparing the diffusion range of liquid CO_2 of the two models in different years, it can be found that the preferential coal mining model produces a large number of water-conducting fractures in the overlying rock after coal seam excavation, which causes varying degrees of changes in the permeability and porosity of the overlying rock beneath the uranium mine so that the migration

ISSN: 2472-3703 DOI: 10.6911/WSRJ.202304_9(4).0031

speed and diffusion range of liquid CO_2 in this model are much greater than those in the preferential uranium mining model.

5.1.2 Gaseous CO_2 transport

In the first year of the simulation, the diffusion range of gaseous CO2 in the two models mainly existed at 10-30m inside the uranium ore layer. With the increase of the simulation time, gaseous CO2 did not significantly diffuse along the ore layer like liquid CO_2 but only generated migration diffusion in the horizontal direction (Fig. 6 and Fig. 7). In the preferential uranium mining model, the gas CO_2 migration effect is low, the diffusion range is still 50m from both sides of the model boundary, and the deepest vertical migration is 10m below the uranium seam. In the preferential coal mining model, the horizontal diffusion effect of gaseous CO_2 is significantly higher, and the migration range in the fifth year has reached the 20-year simulation effect of the preferential uranium mining model. In the 20th year, gaseous CO_2 almost covers the entire uranium ore layer. Rarely is no significant difference in the vertical

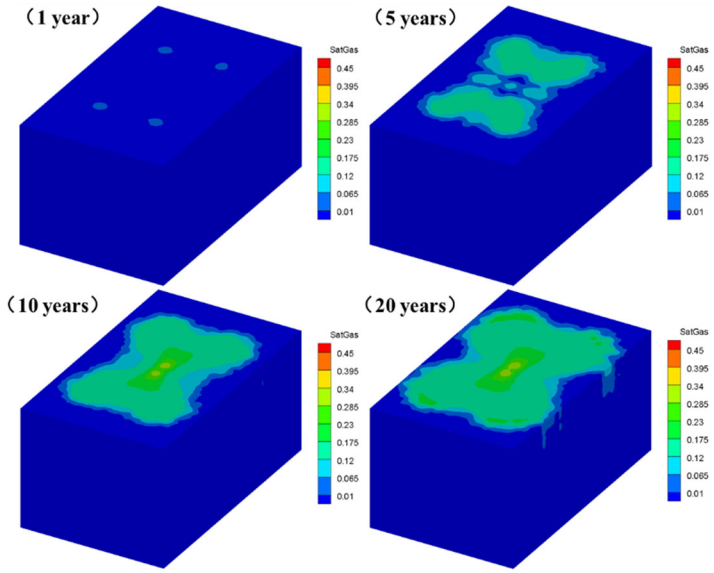

(a)Preferential uranium mining model

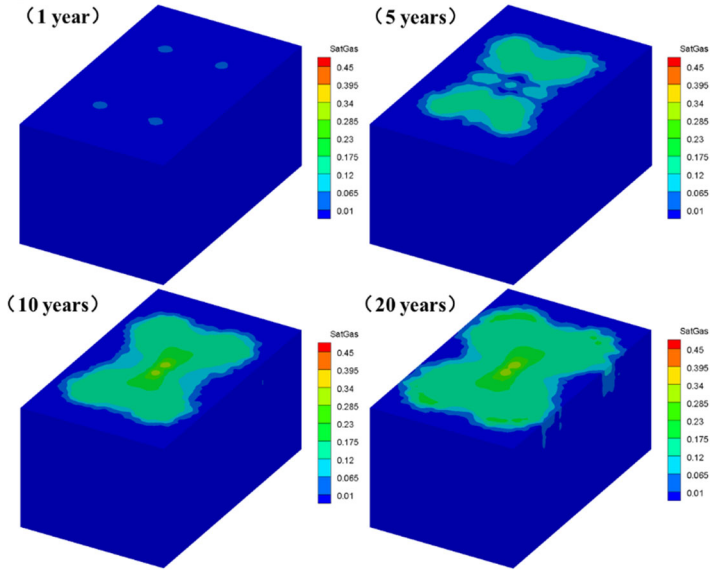

(b)Preferential coal mining model

Figure 6. CO_2 gas saturation in different models

ISSN: 2472-3703 DOI: 10.6911/WSRJ.202304_9(4).0031

migration diffusion range is still 50m from both sides of the model boundary, and the deepest vertical migration is 10m below the uranium seam. In the preferential coal mining model, the horizontal diffusion effect of gaseous CO_2 is significantly higher, and the migration range in the fifth year has reached the 20-year simulation effect of the preferential uranium mining model. In the 20th year, gaseous CO_2 almost covers the entire uranium ore layer. Rarely is no significant difference in the vertical migration range of gaseous CO_2 between the two models.

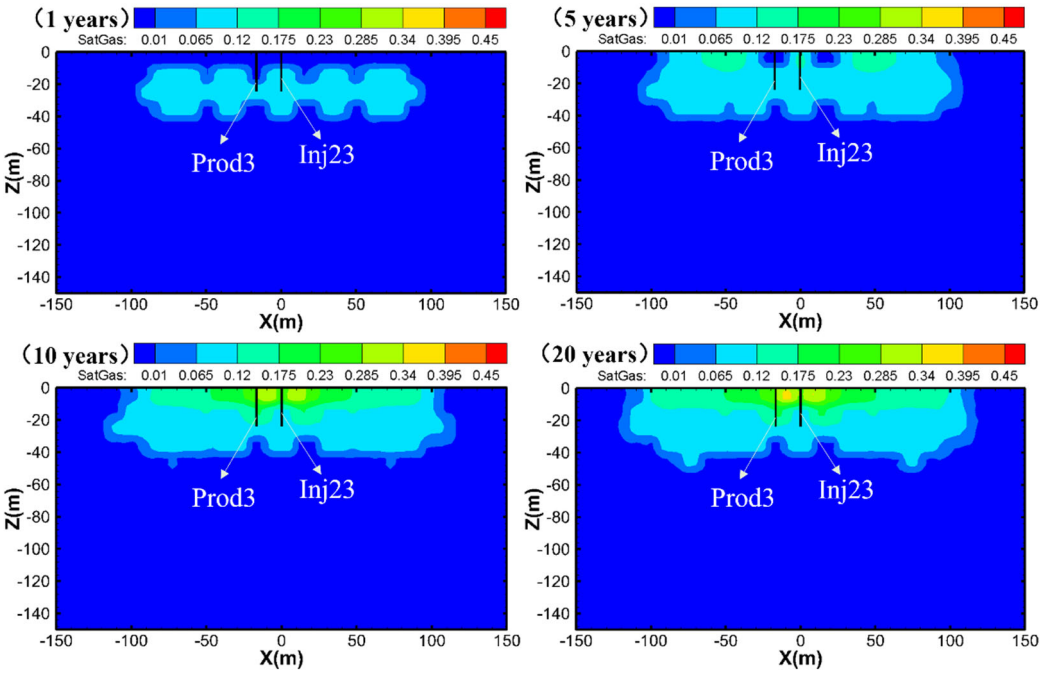

(a)Preferential uranium mining model

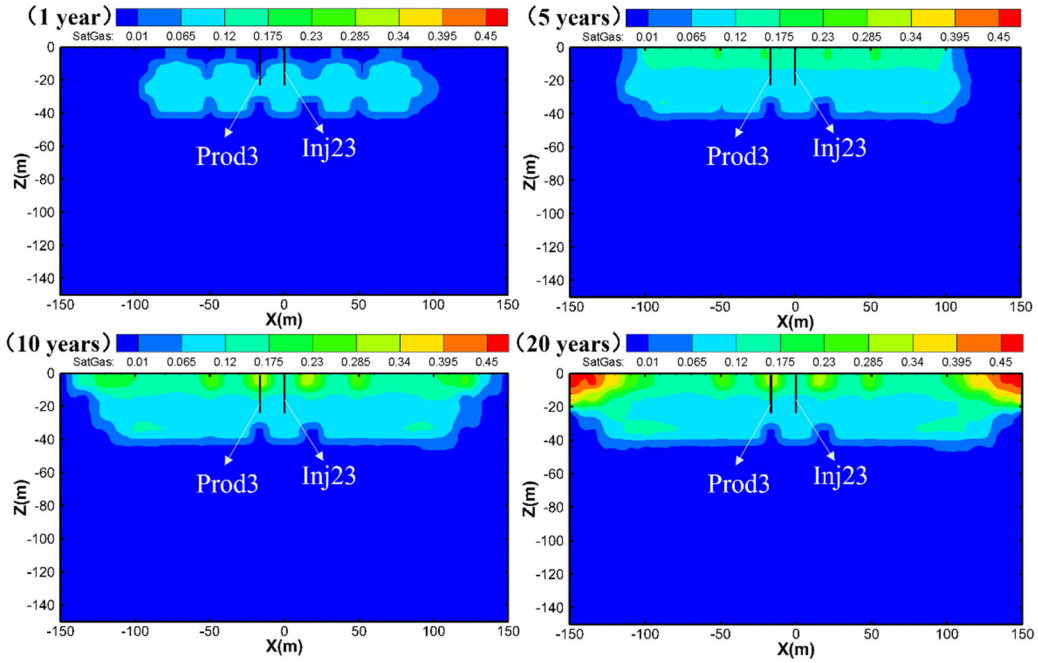

(b)Preferential coal mining model

Figure 7. CO_2 gas saturation Y=90m profile in different models

ISSN: 2472-3703 DOI: 10.6911/WSRJ.202304_9(4).0031

They only spread to about 10m below the uranium layer (Fig. 7). It shows that the sequence of coal seam mining has no significant influence on gaseous CO_2, and gaseous CO_2 is not the main factor affecting the efficiency of uranium ore leaching and pollutant diffusion.

5.2. Mineral chemical reactions and PH

In the process of CO_2+O_2 in-ground leaching, with the operation of pumping wells and injection wells, minerals in the reservoir will be dissolved and precipitated, and some fine colloidal particles in groundwater will also be deposited in the circulation channel during migration to form a mineral blockage, thus affecting the leaching efficiency of uranium ore. The essential colloidal particles are SiO_2. The PH value of groundwater is the main factor determining its precipitation capacity. Fig 8 shows the PH and HCO_3^- concentration changes of production well Prod3 and injection well Inj23 in different models (in data processing, it was found that the PH of each injection well and each pumping well, and the change rule and value of representative ion concentration were consistent, so only Prod3 and Inj23 were selected for analysis), among which HCO_3^- ion concentration was the leading cause of PH change. The relevant chemical reaction formula is as follows:

$$CO_2 + H_2O \rightleftharpoons H^+ + CO_3^{2-} \quad (6)$$

$$CO_3^{2-} + CO_2 + H_2O = 2HCO_3^- \quad (7)$$

$$HCO_3^- + H_2O \rightleftharpoons H_2CO_3 + OH^- \quad (8)$$

The PH value and the concentration of HCO_3^- at Inj23 of the two models are almost the same. The PH value decreases from 4.5 to 3.1 in the simulation's first two years, and the HCO_3^- concentration increases first and then fluctuates. The peak molar concentration reached 1.8mol/kg (Fig. 8b). Since CO_2 has been injected into the ore layer through the injection well, CO_3^{2-} reacts with CO_2 to generate HCO_3^-, and the CO_3^{2-} is constantly consumed so that chemical reactions 4-6 in the aquifer will proceed in the direction of positive response. When the mass fraction of HCO_3^- in groundwater is close to saturation, the reaction tends to equilibrium, and the PH of groundwater tends to be constant. In Prod3 of the extraction well, the PH value and concentration of HCO_3^- of the two models are the same. The PH value of the two models rises to 5.3 and 5.55, respectively, showing a trend of first increasing, then decreasing, and finally becoming stable (Fig. 8a), indicating that CO_2 is mainly concentrated near the injection well in the early stage of in-ground leaching. The HCO_3^- generated near the liquid injection moves in the direction of the fluid pumping well. The hydrolysis reaction occurs at the liquid pumping well temporarily shrinks the PH. The continuous increase of CO_2 concentration in the groundwater generates many carbonic acids. The carbonic acid is ionized to produce hydrogen ions, and the PH decreases accordingly. The difference is that the PH peak of the preferential coal mining model is 0.25 higher than that of the model with uranium before coal, and it falls to equilibrium later. The concentration of HCO_3^- in the model with uranium before coal reaches a peak one year earlier than that of the model with coal before uranium indicates that the permeability of the rock layer below the uranium seam increases after the coal seam is mined first. There is more HCO_3^- in the vertical direction, so the concentration of HCO_3^- in the extraction well reaches its peak later.

ISSN: 2472-3703 DOI: 10.6911/WSRJ.202304_9(4).0031

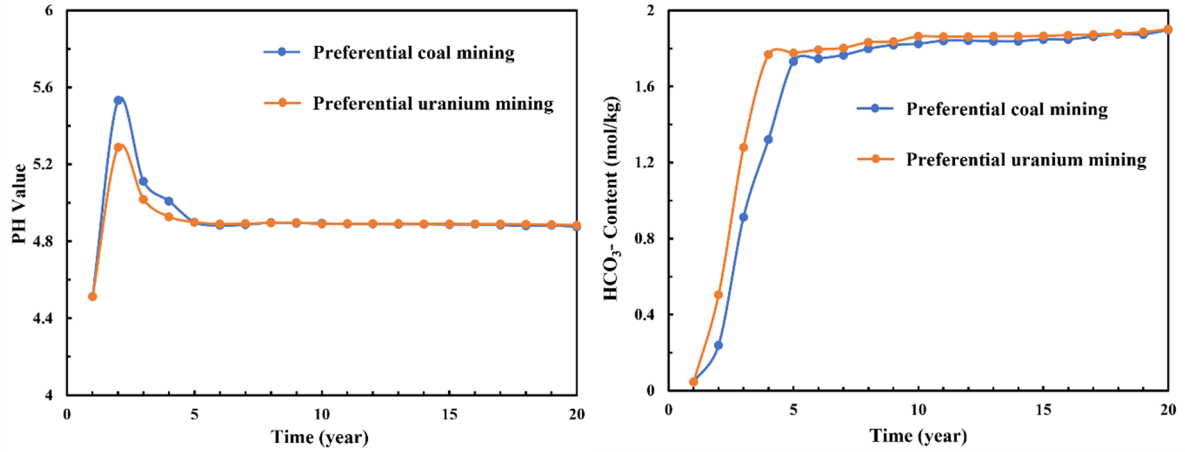

(a) PH and HCO_3^- concentration changes at Prod3 well

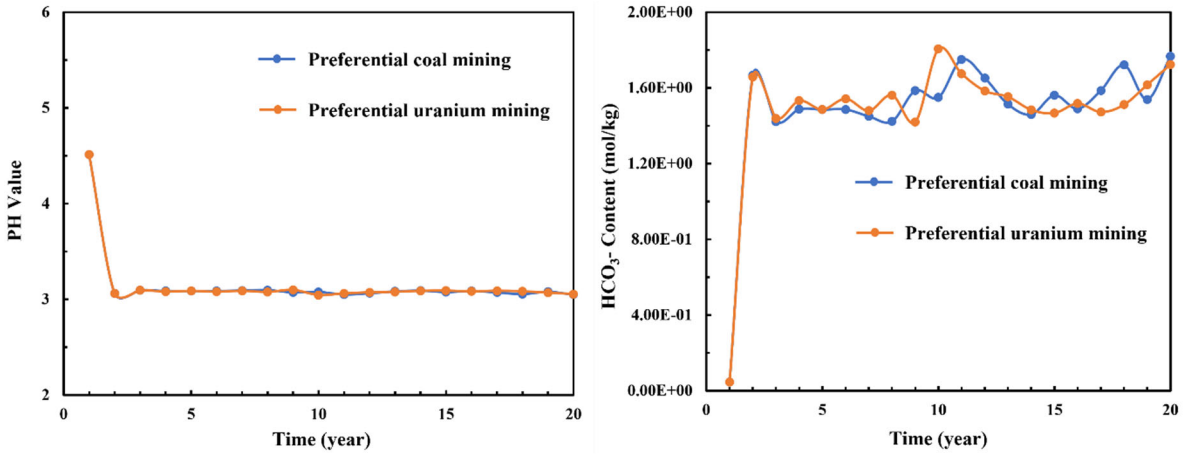

(b) PH and HCO_3^- concentration changes at Inj23 well

Figure 8. CO_2 gas saturation Y=90m profile for different models

With the increase of simulation time, SiO_2 colloidal particles mainly diffuse around the liquid injection well, and the rise of quartz minerals near the fluid injection well is almost 0 (Fig. 9). According to the PH change curve (Fig. 8b), the PH near the liquid injection well is small. However, the PH of the existing environment of SiO_2 colloid needs to be maintained at about 9-10, so it is challenging to generate SiO_2 colloid precipitation around the injection well. At the same time, an outward diffusion flow field is formed between the injection well and the pumping well. The SiO_2 colloid microparticles generated under the condition of high PH also move and diffuse outward with the leaching solution and gradually precipitate. As a result, the mass fraction of quartz minerals near the pumping well and the periphery of the well site is relatively large, while there is almost no quartz mineral formation around the injection well. The change value and law of SiO_2 colloid concentration in Inj23 of the two models are the same, which decreases linearly with the simulation, and the concentration drops to 0 in the second year (Fig. 10b), which is entirely consistent with the PH law at the injection well. The change rule of SiO_2 colloid concentration at Prod3 of the pumping well of the two models is almost the same (Fig. 10a), which can be divided into two stages: it is in a rapid decline trend from 0 to 8 years, and it is in a slight decrease and tends to be stable from 9 to 20 years, which is also almost consistent with the change rule of PH at Prod3 of the pumping well. It shows that the concentration of SiO_2 colloid is highly sensitive to the change in PH value and has a positive correlation. The difference is that the SiO_2 colloid concentration at Prod3 of the pumping well of the preferential coal mining model is always at a higher position than that of the preferential uranium mining model.

ISSN: 2472-3703 DOI: 10.6911/WSRJ.202304_9(4).0031

5.3. Leaching efficiency of uranium

The CO_2 leaching solution injected into the ore layer will cause a series of geochemical reactions, and some ions will precipitate after the response, which will cause the porosity and

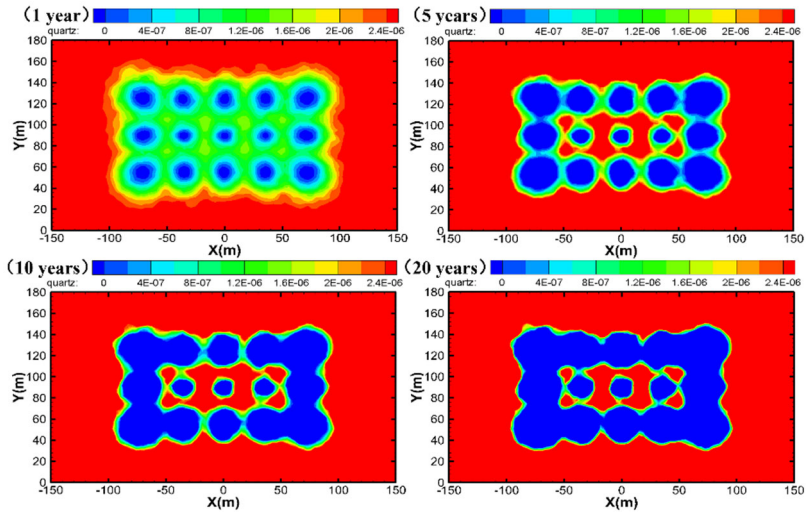

(a) Preferential uranium mining model

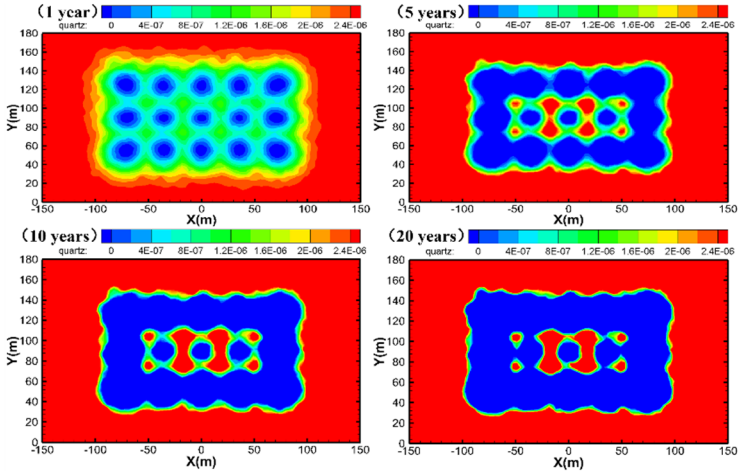

(b) Preferential coal mining model

Figure 9. Variation of quartz mineral volume fraction in different models Z=-30m profile

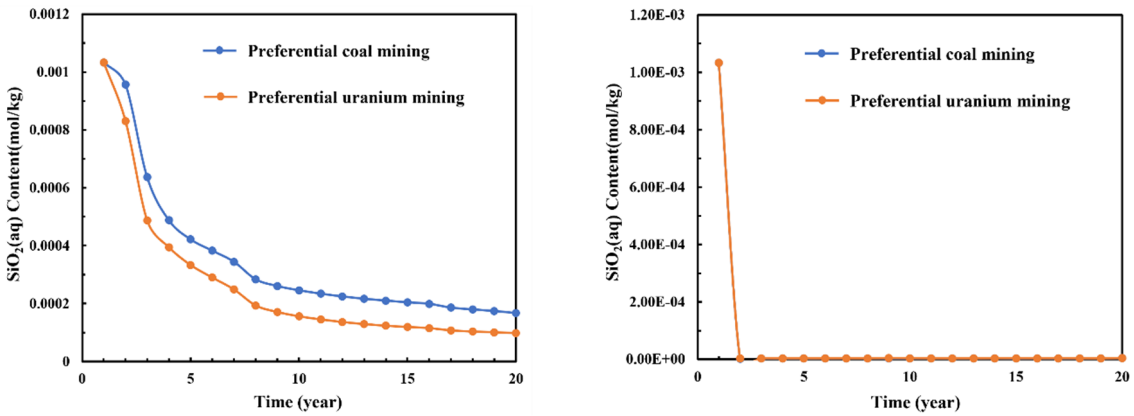

(a) Prod3 well (b) Inj23 well

Figure 10. The change of SiO_2(aq) concentration in different model pumping Wells

ISSN: 2472-3703 DOI: 10.6911/WSRJ.202304_9(4).0031

permeability of the ore layer to change, and then affect the leaching efficiency of uranium ore in the process of in-situ leaching. In the extraction well, the change rule of uranium concentration in the leached solution of the two models is the same (Fig. 11a).

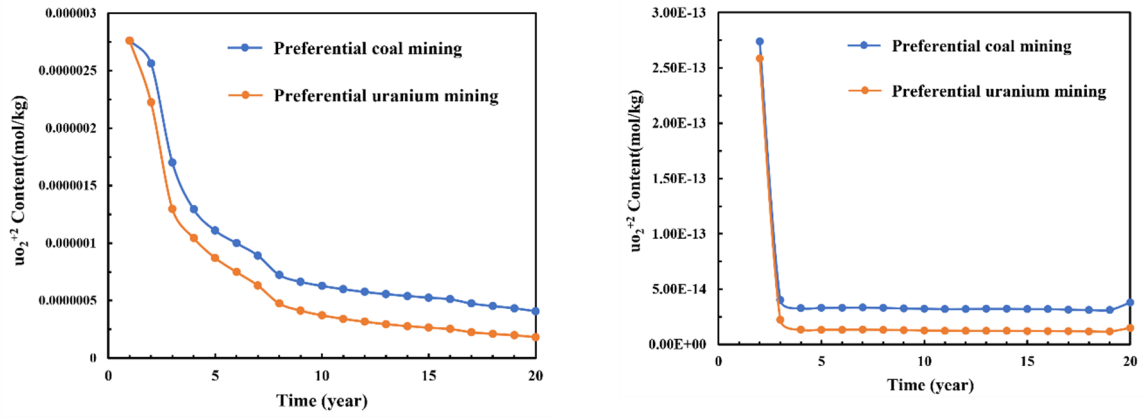

(a) Prod3 well (b) Inj23 well

Figure 11. The change of UO_2^{+2} concentration in different model pumping Wells

0-8 years is the main period of uranium ore leaching, and the uranium concentration in the leached solution is the highest in the first year. Most of the uranium in the ore layer is filtered in this period. The difference between the two models is that the uranium concentration of the leaching solution in the preferential coal mining model is always higher than in another model after the first year, indicating that the pores and fractures generated by coal seam mining enhance the circulation ability of the leaching solution in the reservoir, which makes the leaching area more prominent and the uranium recovery rate higher. Fig 11b shows the change in uranium concentration in the injection wells of different models. It can be seen that the change law of uranium concentration at the well point of the two models is almost the same, which decreases straight after the second year and remains stable at a low level after the third year.

5.4. Migration of uranium leaching solution

The change of porosity and permeability of the overlying rock caused by coal seam mining will lead to the evolution of the migration characteristics of uranium-containing leaching solution in the vertical direction, which will directly affect the leaching efficiency of the upper uranium ore. The migration law of uranium-containing leaching solution in different mining sequence models of coal and uranium is studied to ensure the efficient mining of uranium ore and the safe and scientific mining of coal resources. At the beginning of the simulation, the ore layer around the injection well was first contacted with the leaching solution, and the surrounding uranium-bearing minerals began to dissolve, forming uranyl carbonate ions to migrate to the direction of the pumping well. The uranium-bearing minerals around the injection well were gradually exhausted, and the concentration decreased significantly. With the leaching process, the leaching liquid continuously diffuses to the surrounding area, and more uranium minerals in the uranium ore layer dissolve into the ore layer water, forming a "uranium hole" around the injection well. The pressure difference between the pumping well and the injection well constitutes a unique annular flow form in which the ore layer water continuously moves to the pumping well, and the leaching liquid replenishes to the surrounding area (Fig. 12).

ISSN: 2472-3703 DOI: 10.6911/WSRJ.202304_9(4).0031

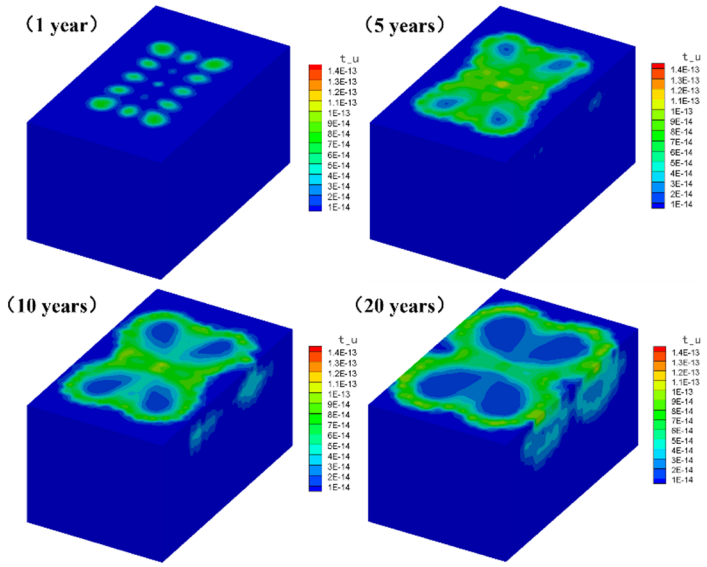

(a) Preferential uranium mining model

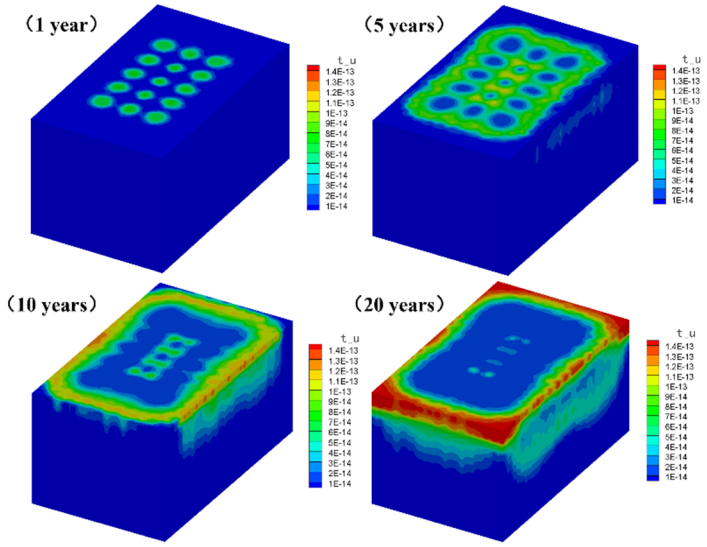

(b) Preferential coal mining model

Figure 12. Istribution of uranium-containing leaching solution in different models

In the preferential uranium mining model, the uranium-containing leach solution diffuses slowly. In the horizontal direction, it spreads to 50m from the model boundary in the first year, 25m from the model boundary in the fifth year, 20m from the model boundary in the tenth year, and 10m from the model boundary in the twentieth year. In the vertical direction, the deepest diffusion is 20m below the uranium ore layer in the first year, the most profound distribution is 30m below the uranium ore layer in the fifth year, and the depth of diffusion is almost unchanged in the 10th year. The deepest diffusion is 40m below the uranium ore layer in the 20th year and 50m away from the coal seam below (Fig. 12a, Fig. 13a).

When the coal seam is mined in priority, the water-conducting cracks under the uranium seam greatly accelerate the migration speed of the leaching solution. In the fifth year of the simulation, the migration and diffusion range of uranium-containing leaching solution in the horizontal and vertical directions reached the diffusion scale in the 20th year of the preferential uranium mining model. In the 20th year of simulation, the leachate diffused to the model's boundary and covered the whole uranium seam in the horizontal direction. In the vertical order, the maximum depth of the leaching solution diffusion reaches 73m below the uranium seam,

ISSN: 2472-3703 DOI: 10.6911/WSRJ.202304_9(4).0031

which is only 17m away from the coal seam, increasing by 33m compared with the maximum migration depth of the uranium first and coal later model, forming a "bipod" shaped migration field (Fig. 12b, Fig. 13b).

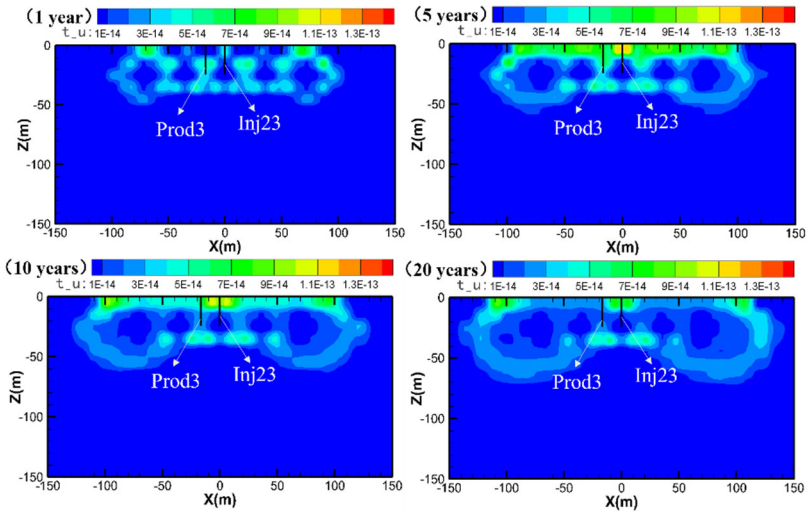

(a) Preferential uranium mining model

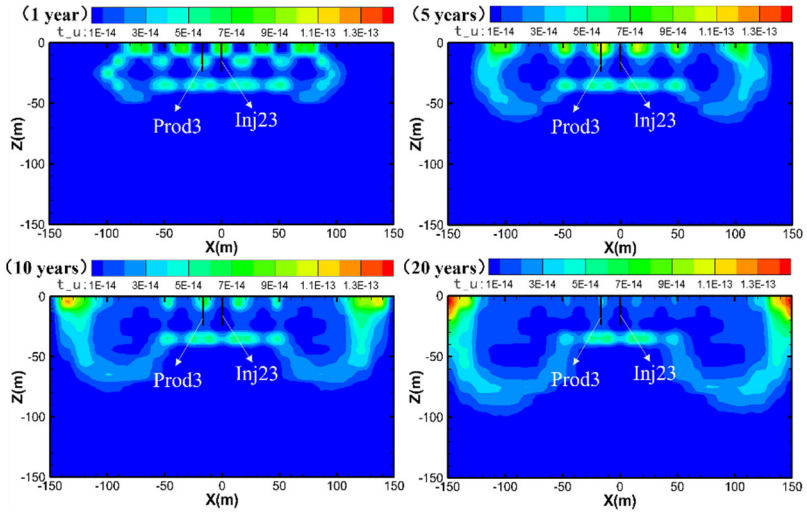

(b) Preferential coal mining model

Figure 13. Istribution of uranium-containing leaching solution Y=90m profile

6. CONCLUSION

(1) The diffusion range of liquid CO_2 in the fifth year during coal-first uranium has reached the maximum diffusion range in the preferential uranium mining model. By the 20th year of the simulation, liquid CO_2 has spread to cover the entire uranium ore layer, and the maximum vertical migration depth has reached 75m below the uranium ore layer. It is only 15m away from the coal seam below, which is 30m higher than the maximum vertical migration depth of the preferential uranium mining model.

(2) The water-conduction fracture field generated below the uranium seam greatly accelerates the migration speed of the leaching solution under the scenario of coal mining preferential. In the fifth year of the simulation, the migration and diffusion range of the uranium-containing leaching solution in the horizontal and vertical directions reaches the diffusion scale of the 20th year of the preferential uranium mining model. In the 20th year of the simulation, the leaching solution diffuses to the boundary of the model in the horizontal

ISSN: 2472-3703 DOI: 10.6911/WSRJ.202304_9(4).0031

direction. Covering the whole uranium ore layer in the vertical direction, the deepest diffusion of the leaching solution reaches 73m below the uranium ore layer, only 17m away from the coal seam, 33m more than the maximum migration depth of the preferential uranium mining model forming a "bipod" shaped migration field.

(3) The change of leaching time is influenced by the shift in uranium ore recovery rate. 0-8 years is the main period of uranium ore leaching. The concentration of uranium in the leaching solution is the highest in the first year, during which most of the uranium in the ore layer is leached. Between 8-20 years of leaching, the uranium content of the leaching solution decreases slowly and tends to be stable. The recovery rate of uranium resources is higher in the preferential coal mining model, and the uranium leaching solution will not invade the coal seam.

ACKNOWLEDGMENTS

This paper was supported by the Institute of Energy, Hefei Comprehensive National Science Center (Grant No.21KZS216), China; the Open Fund of State Key Laboratory of Water Resource Protection and Utilization in Coal Mining (Grant No. GJNY-18-73.7), China; Collaborative Innovation Project of Colleges and Universities of Anhui Province (Grant No. GXXT-2021- 019), China; the National Youth Science Foundation (Grant No. 51904011), the National Science Foundation (Grant No.52227901), China; Anhui Provincial Natural Science Foundation (Grant No. 1908085QE183), China; the Open Fund of State Key Laboratory of Mining Response and Disaster Prevention and Control in Deep Coal Mines (Grant No. SKLMRDPC19ZZ05), China.

REFERENCES

[1] A. Traverso, R. Bertone and A. F. Massardo, “Transient Modeling of a Rotary-Kiln Hydrolyser”, Journal of Mechanical Engineering, 2007, Vol. 6 (12), p511-523.

[2] Akhtar S, Yang X, Pirajno F, “Sandstone type uranium deposits in the Ordos Basin, Northwest China: A case study and an overview”, Journal of Asian Earth Sciences. 2017, Vol. 146, p367-82.

[3] Zhu Q, Yu Ra, Feng X, et al, “Mineralogy, geochemistry, and fluid action process of uranium deposits in the Zhiluo Formation, Ordos Basin, China”, Ore Geology Reviews Top. 2019, Vol. 111, p102984.

[4] Ziying L, Anping C, Xiheng F, et al, “Origin and Superposition Metallogenic Model of the Sandstone-type Uranium Deposit in the Northeastern Ordos Basin, China”, Acta Geologica Sinica (English Edition). 2008, Vol. 82 (4), p745-9.

[5] Rongxi L, Youzhu L, “The geologic features of mineralization at the Dongsheng uranium deposit in the northern Ordos Basin (Central China)”, Russian Geology and Geophysics. 2011, Vol. 52 (6), p593-602.

[6] Yan T, Wang W, Chen L, et al, “Hydrological effects of the underground hydraulic curtain with different design parameters based on numerical modeling for a co-exploitation of coal and uranium”, International Journal of Coal Geology. 2022, Vol. 257, p104011.

[7] Chen Y, Jin R, Miao P, et al, “Occurrence of pyrites in sandstone-type uranium deposits: Relationships with uranium mineralization in the North Ordos Basin, China”, Ore Geology Reviews. 2019, Vol. 109, p426-47.

[8] Bonnetti C, Malartre F, Huault V, et al, “Sedimentology, stratigraphy and palynological occurrences of the late Cretaceous Erlian Formation, Erlian Basin, Inner Mongolia, People's Republic of China”, Cretaceous Research. 2014, Vol. 48, p177-92.

[9] Hou B, Keeling J, Li Z, “Paleovalley-related uranium deposits in Australia and China: A review of geological and exploration models and methods”, Ore Geology Reviews. 2017, Vol. 88, p201-34.

ISSN: 2472-3703 DOI: 10.6911/WSRJ.202304_9(4).0031

[10] Zhang L, Liu C, Fayek M, et al, "Hydrothermal mineralization in the sandstone–hosted Hangjinqi uranium deposit, North Ordos Basin, China", Ore Geology Reviews. 2017, Vol. 80, p103-15.

[11] Dangelmayr MA, Reimus PW, Wasserman NL, et al, "Laboratory column experiments and transport modeling to evaluate retardation of uranium in an aquifer downgradient of a uranium in-situ recovery site", Applied Geochemistry. 2017, Vol. 80, p1-13.

[12] Nguyen VV, Pinder GF, Gray WG, et al, "Numerical simulation of uranium in-situ mining", Chemical Engineering Science. 1983, Vol. 38 (11), p1855-62.

[13] Fu H, Ding D, Sui Y, et al, "Transport of uranium(VI) in red soil in South China: influence of initial pH and carbonate concentration", Environmental Science and Pollution Research. 2019, Vol. 26 (36), p37125-36.

[14] Windt LD, Burnol A, Montarnal P, et al, "Intercomparison of reactive transport models applied to UO2 oxidative dissolution and uranium migration", Journal of Contaminant Hydrology. 2003, Vol. 61 (1-4), p303-12.

[15] Yabusaki SB, Fang Y, Long PE, et al, "Uranium removal from groundwater via in situ biostimulation: Field-scale modeling of transport and biological processes", Journal of Contaminant Hydrology. 2007, Vol. 93 (1-4), p216-35.

[16] Zhang F, Luo W, Parker JC, et al, "Modeling uranium transport in acidic contaminated groundwater with base addition, Journal of Hazardous Materials". 2011, Vol. 190 (1-3), p863-8.

[17] Phillippi JM, Loganathan VA, McIndoe MJ, et al, "Theoretical Solid/Solution Ratio Effects on Adsorption and Transport: Uranium(VI) and Carbonate", Soil Science Society of America Journal. 2007, Vol. 71 (2), p329-35.

[18] Curtis GP, Davis JA, Naftz DL, "Simulation of reactive transport of uranium(VI) in groundwater with variable chemical conditions", Water Resources Research. 2006, Vol. 42 (4), p1-15.

[19] Lu Y, Wang L, "Numerical simulation of mining-induced fracture evolution and water flow in coal seam floor above a confined aquifer", Computers and Geotechnics. 2015, Vol. 67, p157-71.

[20] Meng L, Feng Q, Li Q, "Coupled simulation–optimization model for draining confined aquifer via underground boreholes to prevent water inrush of coal mines", Environmental Earth Sciences. 2018, Vol. 77 (17), p1-20.

[21] Karaman A, Carpenter P, Booth C, "Type-curve analysis of water-level changes induced by a longwall mine", Environmental Geology. 2001, Vol. 40 (7), p897-901.

[22] Zhang D, Fan G, Ma L, et al, "Aquifer protection during longwall mining of shallow coal seams: A case study in the Shendong Coalfield of China", International Journal of Coal Geology. 2011, Vol. 86 (2-3), p190-6.

[23] Zhang D, Fan G, Liu Y, et al, "Field trials of aquifer protection in longwall mining of shallow coal seams in China", International Journal of Rock Mechanics and Mining Sciences. 2010, Vol. 47 (6), p908-14.

[24] Zhai M, Ma D, Bai H, "Diffusion Mechanism of Slurry during Grouting in a Fractured Aquifer: A Case Study in Chensilou Coal Mine, China", Mathematics. 2022; Vol. 10(8):p1345.

[25] Fan G, Zhang D, "Mechanisms of Aquifer Protection in Underground Coal Mining". Mine Water and the Environment, 2014, Vol. 34 (1), p95-104.

[26] Zhang R, Jiang Z, Zhou H, et al, "Groundwater outbursts from faults above a confined aquifer in the coal mining", Natural Hazards. 2013, Vol. 71 (3), p1861-72.

[27] Cui G, Wei J, Feng X-T, et al, "Preliminary study on the feasibility of co-exploitation of coal and uranium", International Journal of Rock Mechanics and Mining Sciences. 2019, Vol. 123, p104098.

ISSN: 2472-3703 DOI: 10.6911/WSRJ.202304_9(4).0031

[28] Zhang T, Gan Q, Zhao Y, et al, "Investigations into Mining-Induced Stress–Fracture–Seepage Field Coupling Effect Considering the Response of Key Stratum and Composite Aquifer", Rock Mechanics and Rock Engineering. 2019, Vol. 52 (10), p4017-31.

[29] Zhang T, Yuan L, Wei Z, et al, "Coupled Multifield Response to Coordinate Mining of Coal and Uranium: A Case Study", Water. 2020, Vol. 12 (1), p1-14.

[30] Zhang T, He X, Zhang K, et al, "Hydrogeology Response to the Coordinated Mining of Coal and Uranium: A Transparent Physical Experiment", Geofluids. 2021, Vol. 2021, p1-10.

[31] Wang H, Zhang L, Lei H, et al, "Potential for uranium release under geologic CO2 storage conditions: The impact of Fe(III)", International Journal of Greenhouse Gas Control. 2021, Vol. 107, p103266.

[32] Asghar F, Sun Z, Chen G, et al, "Geochemical Characteristics and Uranium Neutral Leaching through a CO2 + O2 System—An Example from Uranium Ore of the ELZPA Ore Deposit in Pakistan", Metals. 2020, Vol. 10 (12), p1-19.

[33] Xu T, Sonnenthal E, Spycher N, et al, "TOUGHREACT—A simulation program for non-isothermal multiphase reactive geochemical transport in variably saturated geologic media: Applications to geothermal injectivity and CO2 geological sequestration", Computers & Geosciences. 2006, Vol. 32 (2), p145-65.

[34] Xu T, Spycher N, Sonnenthal E, et al, "TOUGHREACT Version 2.0: A simulator for subsurface reactive transport under non-isothermal multiphase flow conditions", Computers & Geosciences. 2011, Vol. 37 (6), p763-74.

[35] Mouaouia F, Jean-Luc G, Patrick LQ, "Nonlinear corrections to Darcy's law at low Reynolds numbers", Journal of Fluid Mechanics. 1997, Vol. 343, p331-50.

[36] Dagan G, "The generalization of Darcy's Law for nonuniform flows", Water Resources Research. 1979, Vol. 15 (1), p1-7.

[37] Xie M, Mayer KU, Claret F, et al, "Implementation and evaluation of permeability-porosity and tortuosity-porosity relationships linked to mineral dissolution-precipitation", Computational Geosciences. 2014, Vol. 19 (3), p655-71.

[38] Zhang T, Nie X, Song S, et al, "Modeling Uranium Transport in Rough-Walled Fractures with Stress-Dependent Non-Darcy Fluid Flow", Mathematics. 2022, Vol. 10 (5), p1-21.

[39] Meng Z, Shi X, Li G, "Deformation, failure and permeability of coal-bearing strata during longwall mining", Engineering Geology. 2016, Vol. 208, p69-80.

[40] Chen H, Cheng Y, Ren T, et al, "Permeability distribution characteristics of protected coal seams during unloading of the coal body", International Journal of Rock Mechanics and Mining Sciences. 2014, Vol. 71, p105-16.

[41] Adhikary DP, Guo H, "Modelling of Longwall Mining-Induced Strata Permeability Change", Rock Mechanics and Rock Engineering. 2014; Vol. 48 (1): p345-59.

[42] Özgen Karacan C, Goodman G, "Hydraulic conductivity changes and influencing factors in longwall overburden determined by slug tests in gob gas ventholes", International Journal of Rock Mechanics and Mining Sciences. 2009; Vol. 46 (7): p1162-74.